Supporting Information for

Local Charge Transfer within Covalent Organic Framework and Pt Nanoparticles Promoting Interfacial Catalysis

Yajun He,[a] Guodong Pan,[a] Liuyi Li,*[a] Shenghong Zhong,[a] Lingyun Li,[a] Zheyuan Liu,*[a] and Yan Yu*[a]

[a] Key Laboratory of Eco-materials Advanced Technology, College of Materials Science and Engineering, Fuzhou University, Fuzhou 350108, China.

Email: lyli@fzu.edu.cn; zheyuan.liu@fzu.edu.cn yuyan@fzu.edu.cn.

Table of Contents

Section 1 Materials and Methods..... 2

Section 2 Synthetic Procedures..... 3

Section 3 Supplementary Figures and tables.....7

Section 4 Liquid ^{1}H and ^{13}C NMR spectra of monomers.....20

References.....22

Section 1. Materials and Methods

Materials. All starting materials and solvents, unless otherwise specified, were purchased in high purity from commercial sources and used without further purification. 2,5-bis(benzyloxy)terephthalohydrazideb (BZTH) and 2,5-bis(pyridin-4-ylmethoxy)terephthalohydrazide (PYTH) were synthesized according to the reported procedure.[1]

Characterization. Powered X-ray diffraction (PXRD) patterns were measured in the range of 2θ = 3-40° on DY5261/Xpert3 diffractometer with Cu Kα radiation (λ=1.5406 Å). X-ray photoelectron spectrometry (XPS) was performed on a Thermo ESCALAB 250 spectrometer, using nonmonochromatic Al Kα X-rays as the excitation source and choosing C 1s (284.6 eV) as the reference line. Liquid ^{1}H and ^{13}C NMR spectras were collected on a Bruker Avance III 500MHz NMR in DMSO-d6 at 25 ºC. The solid-state ^{13}C NMR experiments were performed on a Bruker Avance III 600 NMR spectrometer. Thermogravimetric analysis (TGA) was recorded on NETZSCH STA 449C instrument over the temperature range of 30 to 800 °C under nitrogen atmosphere with a heating rate of 10 °C min^{-1}. Nitrogen adsorption and desorption isotherms were measured at 77 K using a ASAP 2460 system. The samples are degassed at 80 ℃ for 12 h before the measurements. Surface areas are calculated from the adsorption data using Brunauer-Emmett-Teller (BET) equation. The pore size distribution was calculated by using the nonlocal density functional theory (NLDFT) method. Field-emission scanning electron microscopy (SEM) was performed on a JEOL JSM-7500F operated at an accelerating voltage of 3.0 kV. Transmission electron microscope (TEM) was obtained with TECNAI G^2 F20. The H_2 gas produced from D_2O isotope experiments was examined by a gas chromatograph-mass spectrometer (GC-MS, Agilent 7890B-5977B).

Theoretical calculation details: The density functional theory (DFT) computations were performed using the Vienna ab initio simulation package (VASP). The interaction between the ionic core and valence electrons was described by the projector augmented wave method (PAW). The total energy convergence and the forces on each atom were set to be lower than 10−6eV and 0.02 eV A−1. Energy cutoff of 520 eV for the plane wave basis set was used for the structure optimization, deformation charge density and Bader charge analysis. A 1×1×1 k-point mesh was used for the Brillouin zone sampling. The Predew-Burke-Ernzerhor functional with generalized gradient approximation was employed to describe the electron exchange and correlation energy.

Section 2. Synthetic Procedures

Synthesis of Diethyl 2,5-bis(pyridin-4-ylmethoxy)terephthalate

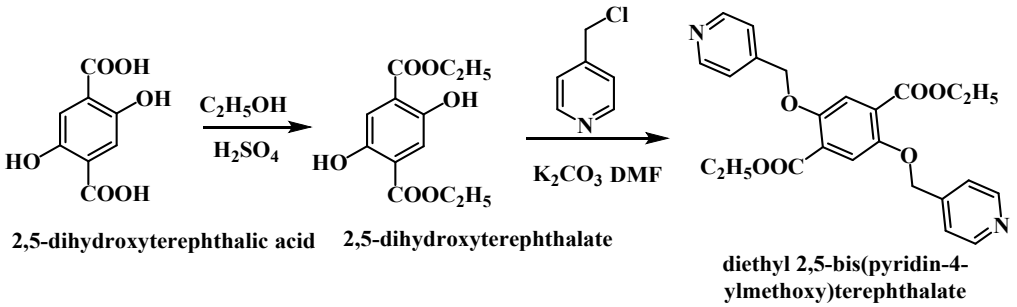

Scheme S1. Synthesis of diethyl 2,5-bis(pyridin-4-ylmethoxy)terephthalate.

A mixture of 2,5-dihydroxyterephthalic acid (3.0 g, 15.1 mmol), concentrated sulfuric acid (5 mL, 93.88 mmol) in ethanol (100 mL) were heated to 80 °C for 15 h. After cooling to room temperature, the mixture was filtered and washed with water to give diethyl 2,5-dihydroxyterephthalate as a yellow-green crystal.

A mixture of diethyl 2,5-dihydroxyterephthalate (1 g) potassium carbonate (5.44 g), 4-(chloromethyl)pyridine (6.46 g) in N,N-dimethylamide (10 mL) was stirred at room temperature for 24 h. After filtration, the filtrate was diluted with

dichloromethane, and then washed 5 times with saturated saline, dried over anhydrous sodium sulfate. After evaporation, the solid was purified by column chromatography on silica gel to give 2,5-bis(pyridin-4-ylmethoxy)terephthalate as a white solid.

Synthesis of 2,5-bis(pyridin-4-ylmethoxy)terephthalohydrazide (PyTH)

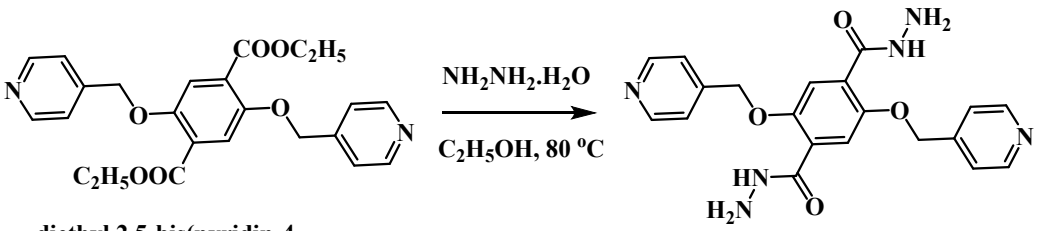

diethyl 2,5-bis(pyridin-4-ylmethoxy)terephthalate

2,5-bis(pyridin-4-ylmethoxy)terephthalohydrazide (PyTH)

Scheme S2. Synthesis of diethyl 2,5-bis(pyridin-4-ylmethoxy)terephthalate

2,5-bis(pyridin-4-ylmethoxy)terephthalate (1g) and hydrazine hydrate (42 mmol, 2.0 mL) were added in absolute ethanol (10 mL). The mixture was stirred and heated at 80 °C for 12 h. After cooling to room temperature, the precipitate was separated by filtration, washed with water and dried to give 2,5-bis(pyridin-4-ylmethoxy)terephthalohydrazide (PYTH) as a white solid.

Synthesis of 2,5-bis(pyridin-4-ylmethoxy)terephthalohydrazide (BzTH)

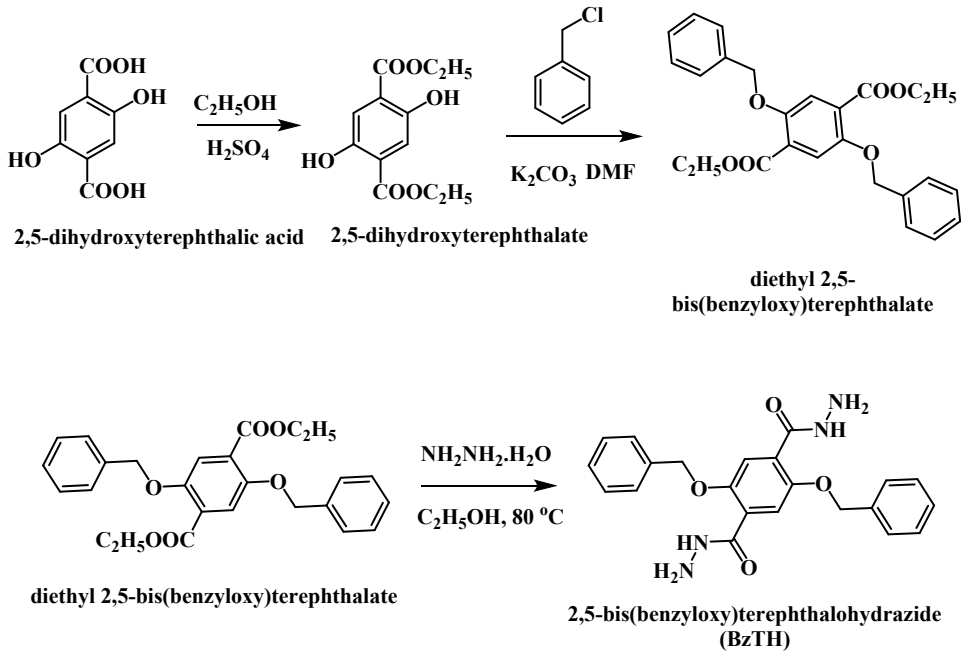

Scheme S3. Synthesis of 2,5-bis(pyridin-4-ylmethoxy)terephthalohydrazide

Following the same procedures as synthesis of PyTH, BzTH was obtained as a white powder. The structure was shown as follows：

Synthesis of Py-COF

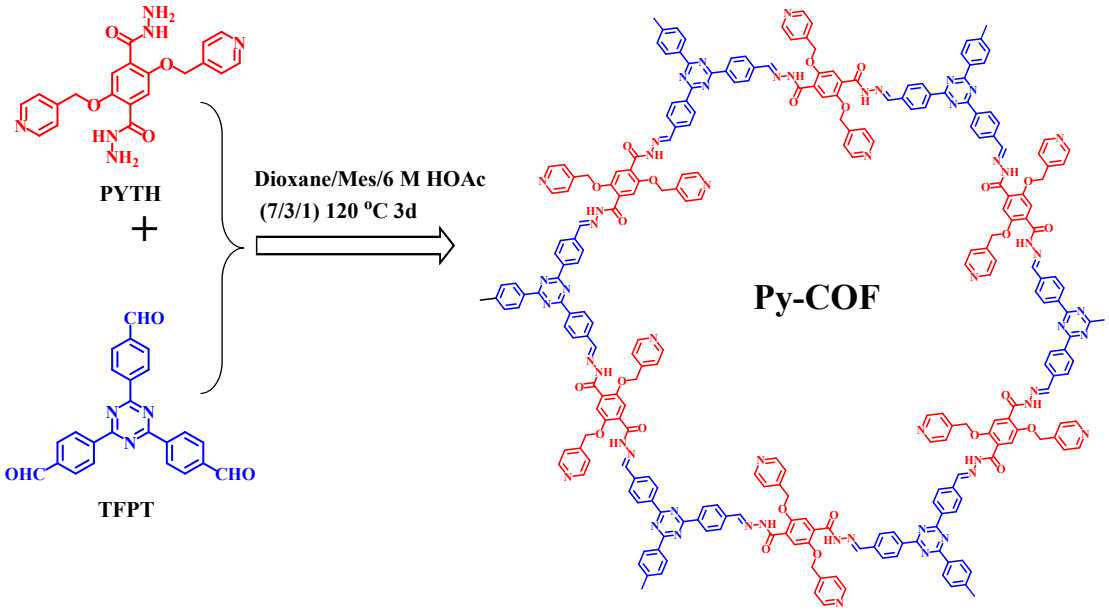

Scheme S4. Scheme of synthesis of Bz-COF.

Synthesis of Bz-COF

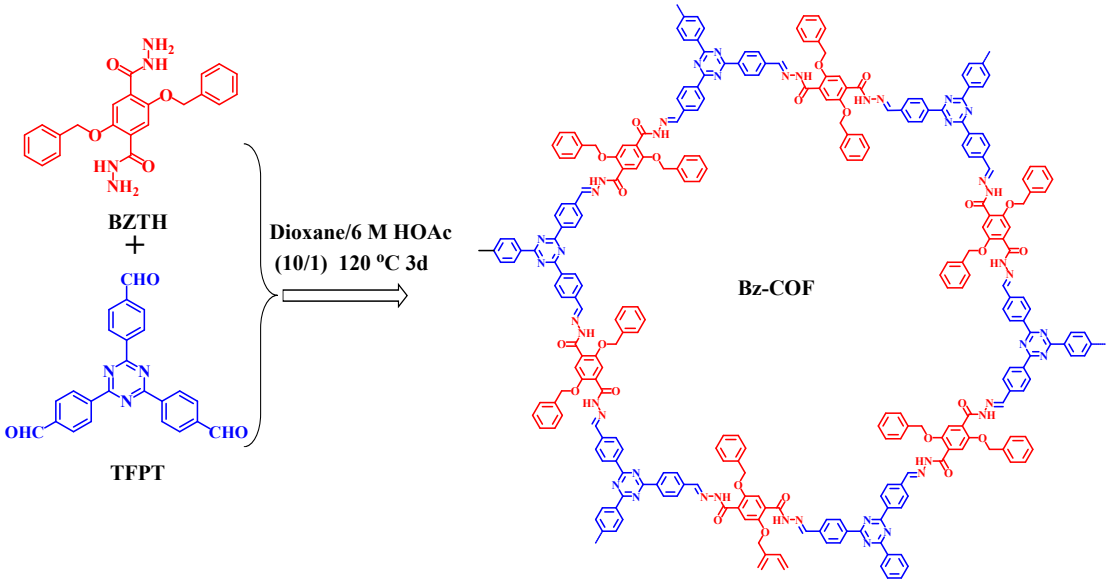

Scheme S5. Scheme of synthesis of Bz-COF.

A Pyrex tube was charged with 2,5-bis(benzyloxy)terephthalohydrazide (BzTH，15.23 mg, 0.0375 mmol), 4,4',4''-(1,3,5-triazine-2,4,6-triyl)tribenzaldehyde TFPT(9.83mg, 0.025mmol), 1,4-dioxane, (1mL) and aqueous acetic acid (0.1 ml, 6 M). This mixture was homogenized by sonication for 15 min and degassed by three freeze-pump-thaw cycles. The tube was sealed and heated at 120 °C for 3 days. The yellow precipitate was collected by centrifugation and washed three times with anhydrous THF, acetone and methanol. The yellow powder was dried at 60 °C under vacuum overnight to yield the Bz-COF (20 mg, 81% yield).

Section 3. Supporting Fig.s and tables.

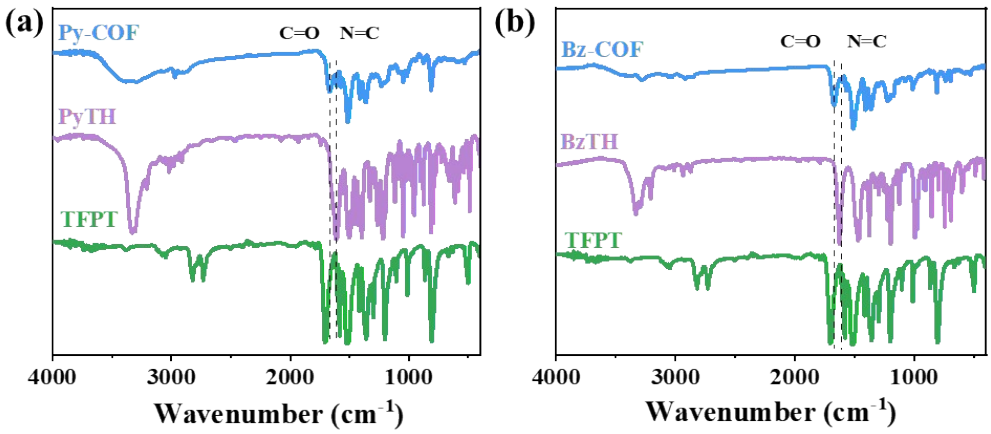

Fig. S1. FT-IR spectra for Py-COF (a), Bz-COF (b) and their monomers.

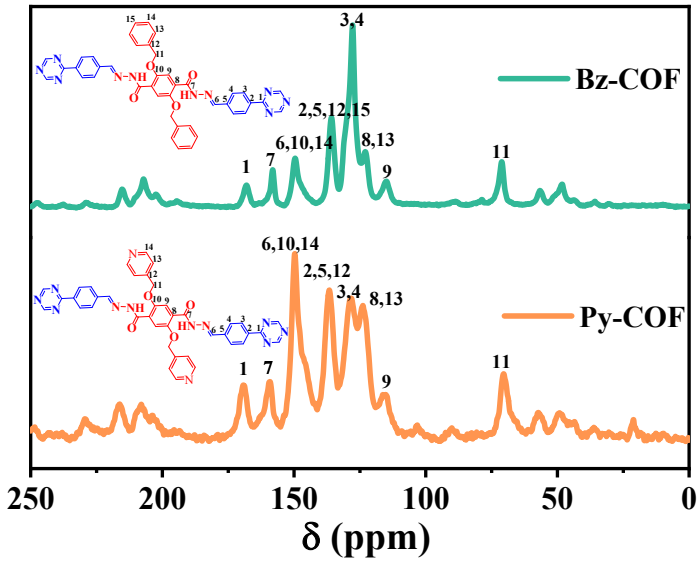

Fig. S2. Solid state ^{13}C NMR spectrum of Py-COF and Bz-COF.

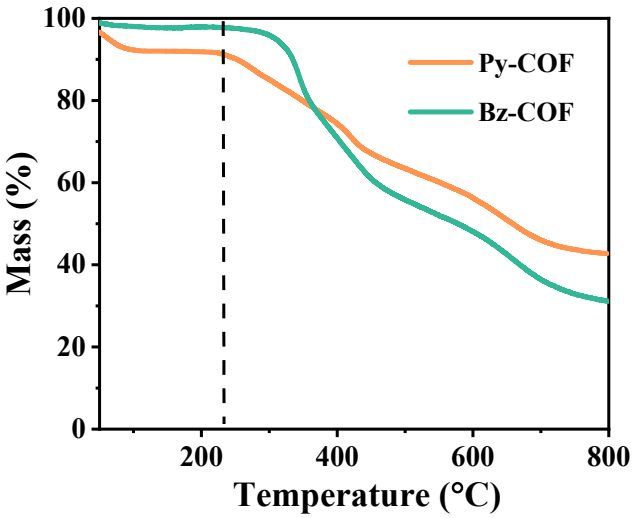

Fig. S3. TGA data of Py-COF and Bz-COF.

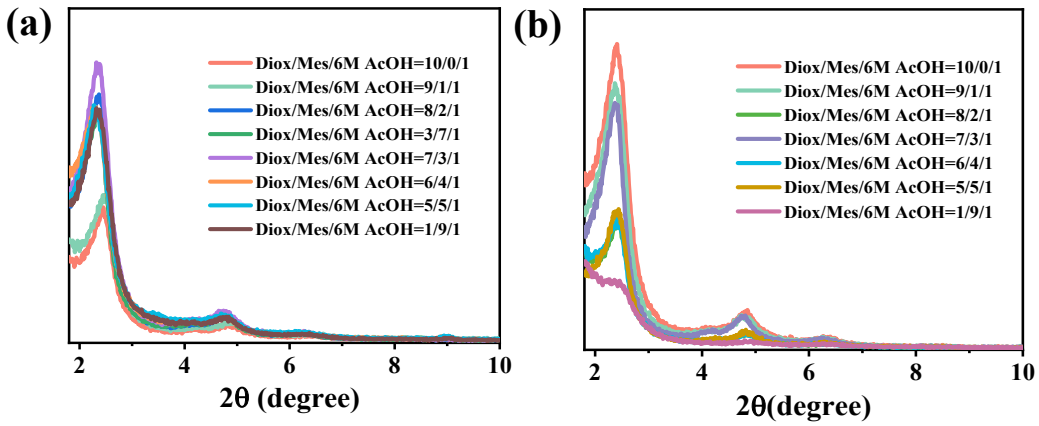

Fig. S4. PXRD patterns of Py-COF (a) and Bz-COF (b) synthesized under different solvent conditions.

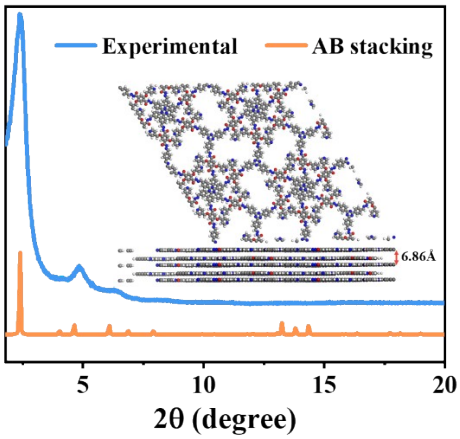

Fig. S5. PXRD patterns of experimental and simulated Py-COF and Pt@Py-COF. Inset: top and side views of the AA stacking structure of Py-COF (red, O; blue, N; gray, C).

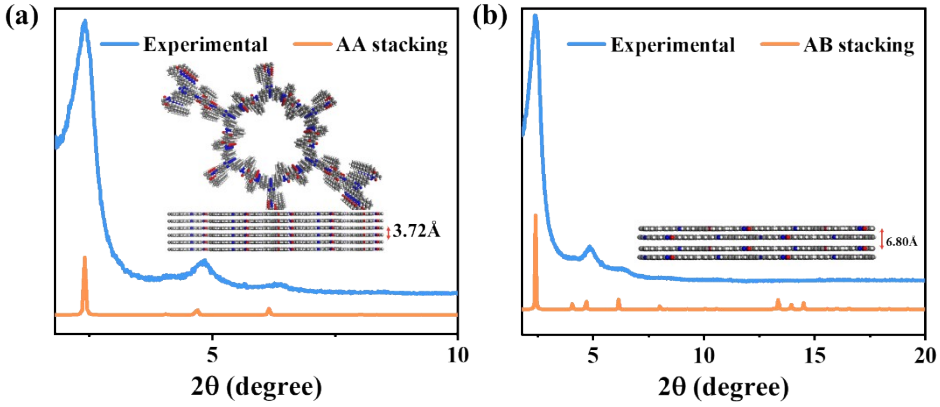

Fig. S6. PXRD patterns of experimental and simulated Bz-COF. Inset: top and side views of the AA stacking (a) and AB stacking structure (b) of Bz-COF (red, O; blue, N; gray, C).

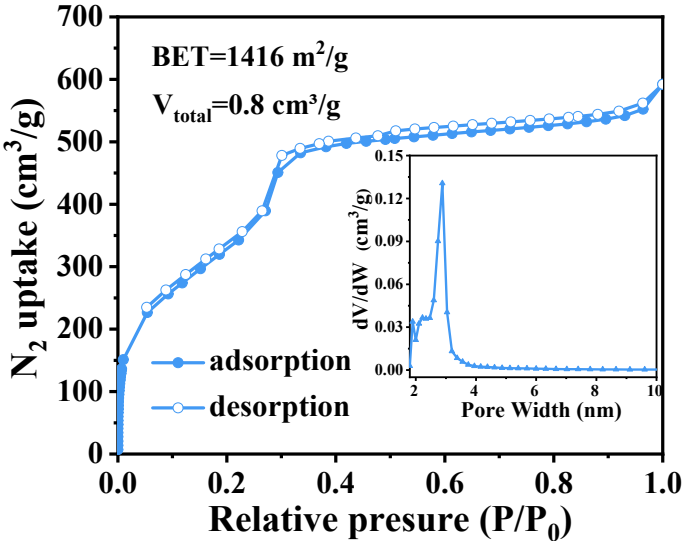

Fig. S7. N_2 adsorption-desorption isotherms of Bz-COF at 77 K (Inset: pore size distribution).

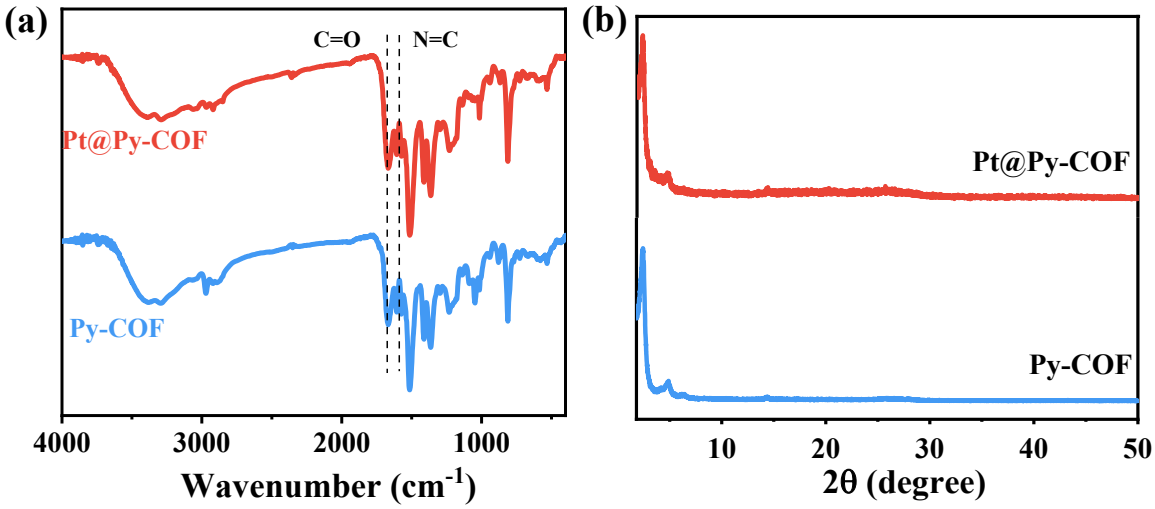

Fig. S8. FT-IR spectra (a) and PXRD patterns (b) of Py-COF and Pt@Bz-COF.

The characteristic peaks of Pt NPs in PXRD patterns were not observed mainly because of the small size, low loading and well dispersibility of Pt NPs in the COF, as shown in TEM, XPS and ICP analyses.

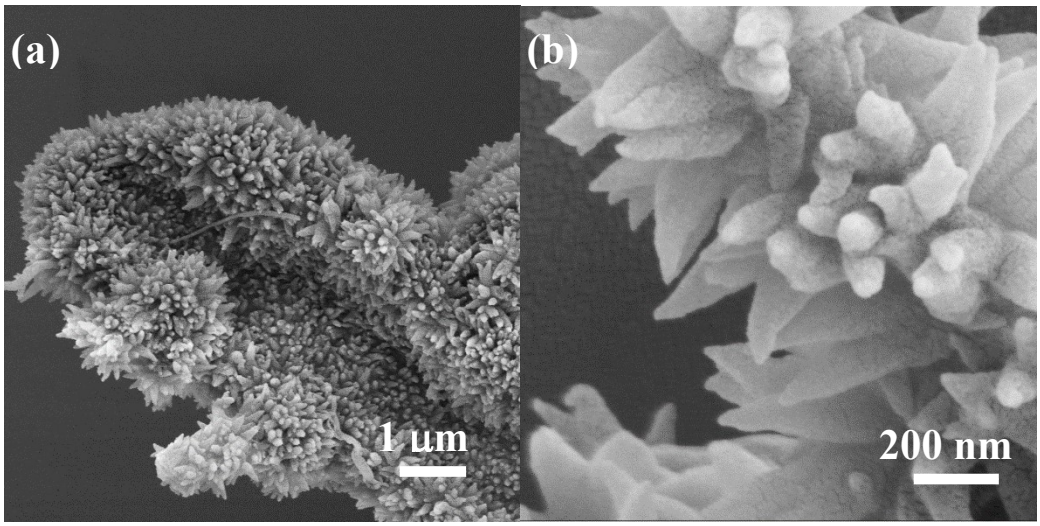

Fig. S9. SEM images of Py-COF (a) and Pt@Py-COF (b).

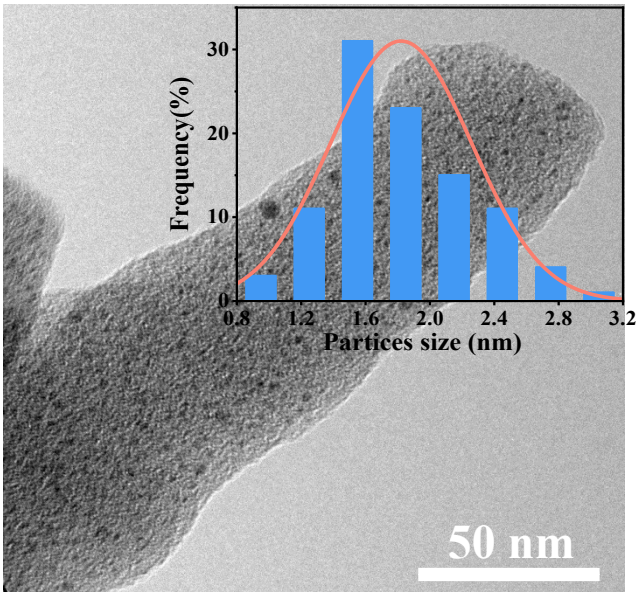

Fig. S10. TEM image of Pt@Py-COF. Inset is the size distribution of Pt NPs

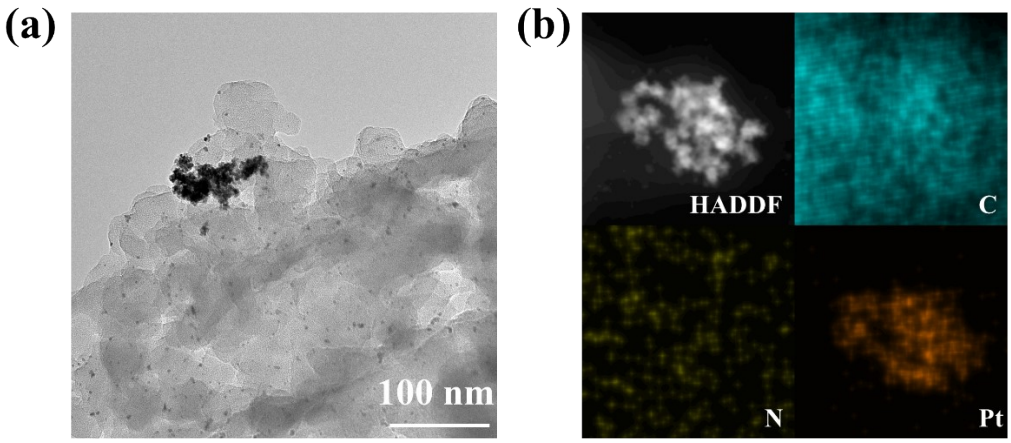

Fig. S11. TEM (a) and EDX elemental mapping (b) images of Pt@Bz-COF.

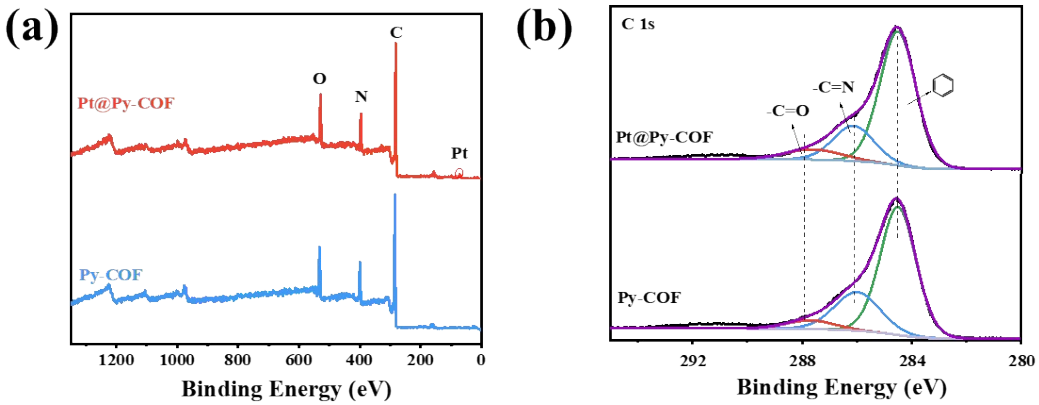

Fig. S12. XPS survey (a) and C 1s XPS spectrum of Py-COF and Pt@Py-COF.

Table S1. Pt chemical state ratio (%) calculated from the Pt 4f XPS spectra of various photocatalyst samples.

	Pt^0	Pt^{2+}
Pt@Py-COF	77.6%	22.4%
Pt@Bz-COF	82.0%	18.0%

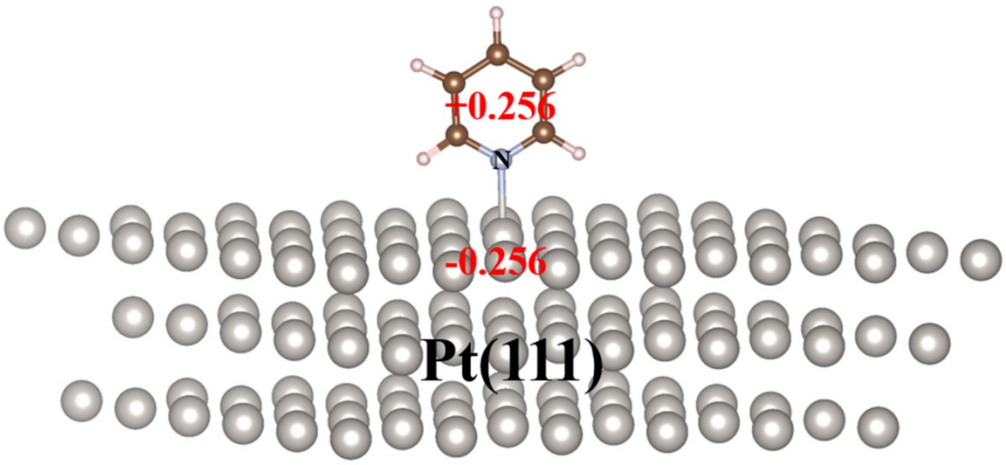

Fig. S13. Bader charge analysis of model of Pt@Py-COF unit. The values in parentheses are corresponding bader charges of Pt nanoparticles and pyridine unit.

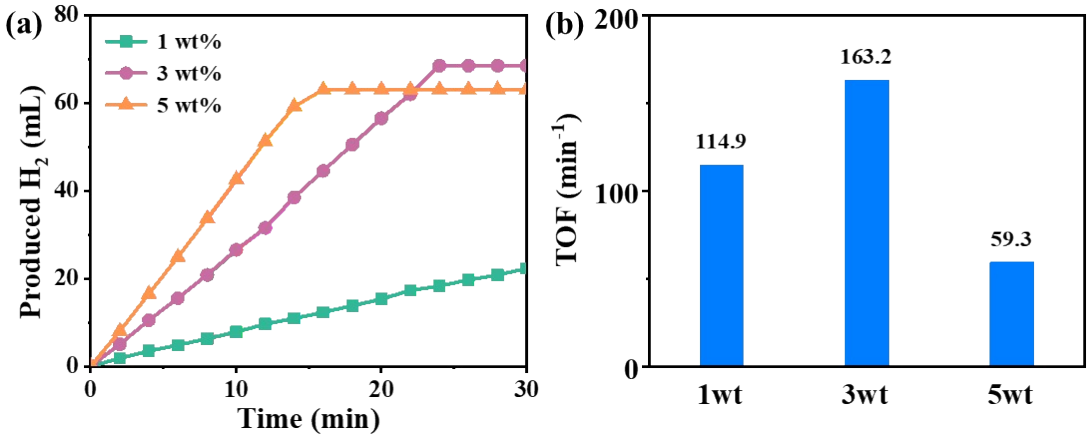

Fig. S14. Kinetics (a) and corresponding TOF (b) of H_2 evolution from NH_3BH_3 over Pt@Py-COF with different platinum loading (Theoretical addition: 1, 3, 5 wt%; Actual loading: 0.55,1.56, 2.31wt%).

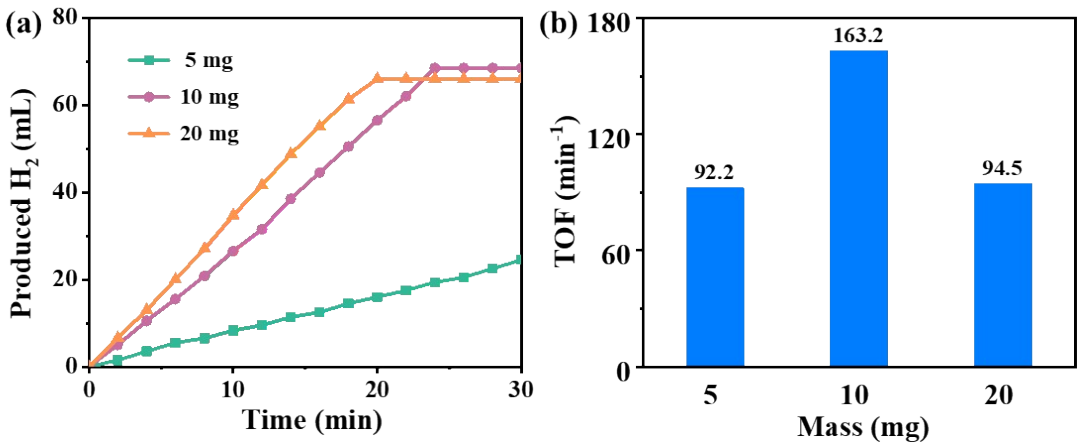

Fig. S15. Kinetics (a) and corresponding TOF (b) of H_2 evolution from AB over different mass of Pt@Py-COF (1.56 wt% Pt@Py-COF: 5, 10 and 20 mg).

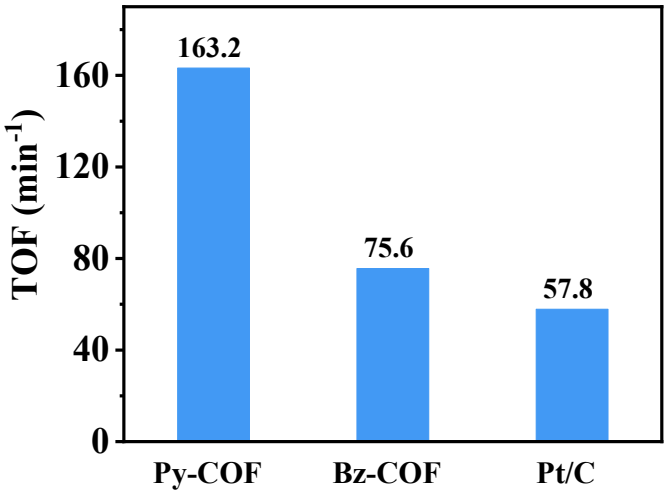

Fig. S16. TOF of H_2 evolution from NH_3BH_3 over Pt@Py-COF, Pt@Bz-COF and commercial Pd/C under the identical conditions (with the conditions of catalysts 10mg, AB 31mg, DI water 5mL and reaction temperature 25℃).

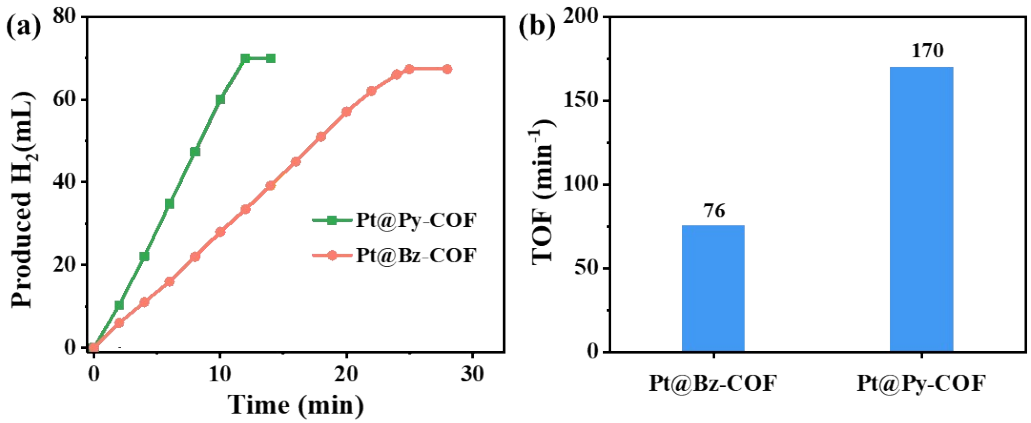

Fig. S17. TOF of H_2 evolution from NH_3BH_3 over Pt@Py-COF and Pt@Bz-COF under same Pt loading (with the conditions of catalysts 10mg, AB 31mg, DI water 5mL, 3wt% Pt loading and reaction temperature 25℃).

Table S2. The catalytic activity of the Pt@Py-COF nanocatalyst compared with other reported Pt NPs based catalysts for the catalytic hydrolysis of AB.

catalyst	T(°C)	catalyst/AB (molar ratio)	TOF (min^{-1})	Ea ($kJmol^{-1}$)	reference
Pt/C	25	0.018	110	-	1
Pt/γ-Al_2O_3	25	0.018	222	21	2
Pt/SiO_2	25	0.018	33	-	2
BOPs@Pt	25	-	131	44	3
Pt@PC-POPs	25	0.016	56	56	4
Pt/CNT-graphene	25		135	35	5
Pt/CNT(1.5 wt%Pt)	30	-	165	38	6

Core–shell Pt@SiO_2	25	0.0024	159	54	[7]
Pt@CF-12	30	0.03	139	31	[8]
Pt@Bz-COF	25	0.00014	75.6	-	This work
Pt@Py-COF	40	0.0005	460	56	This work
Pt@Py-COF	25	0.0008	163	56	This work

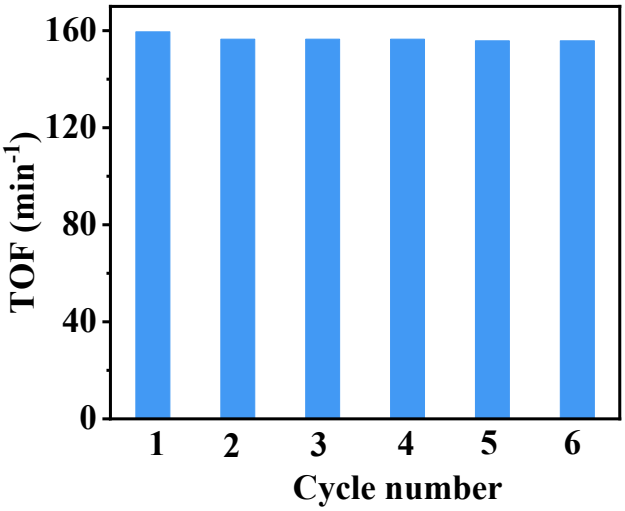

Fig. S18. TOF of H_2 evolution from NH_3BH_3 over recovered Pt@Py-COF washed by 0.1 M HCl at cyclic experiment. (catalysts 10 mg, AB 15.5 mg, DI water 5mLand reaction temperature 25℃).

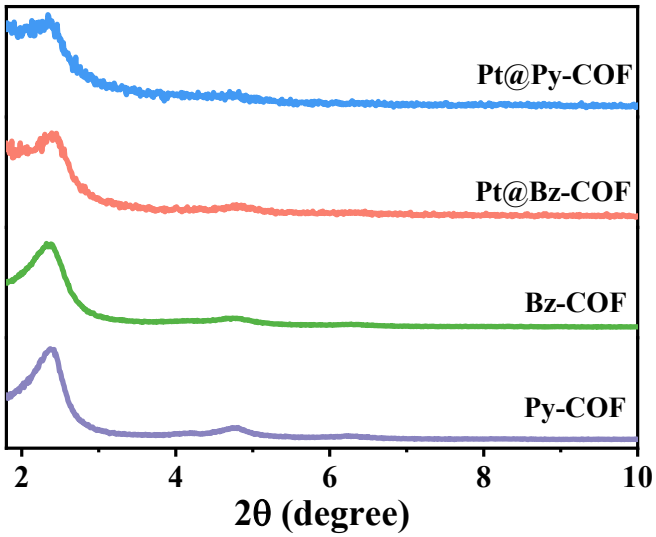

Fig. S19. PXRD patterns of Py-COF, Bz-COF, Pt@Py-COF and Pt@Bz-COF after immersing in 0.1 M HCl for two hours.

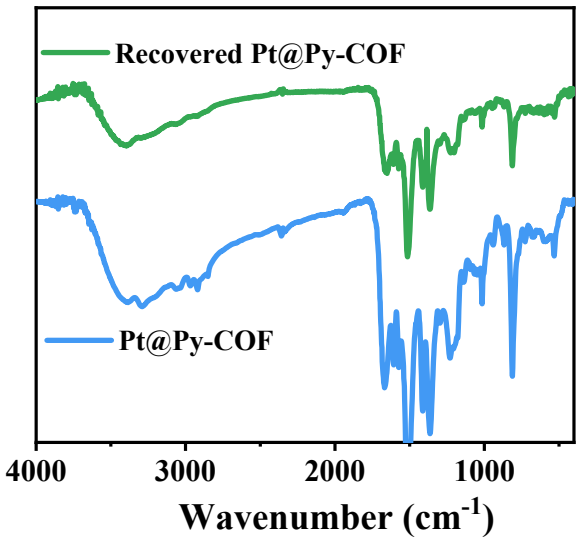

Fig. S20. FT-IR of recovered Pt @ Py-COF from recycling experiment.

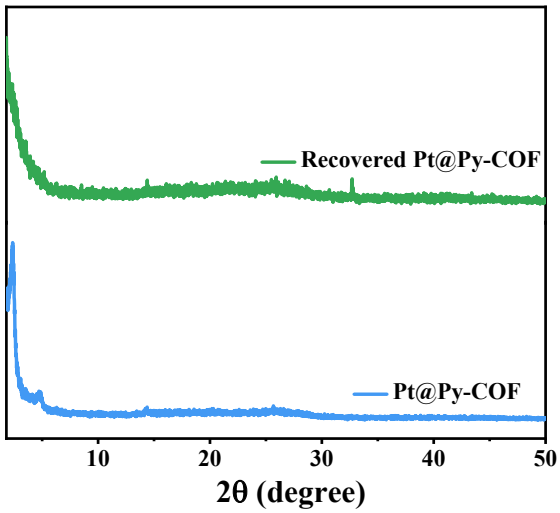

Fig. S21. PXRD patterns of recovered Pt @ Py-COF from recycling experiment.

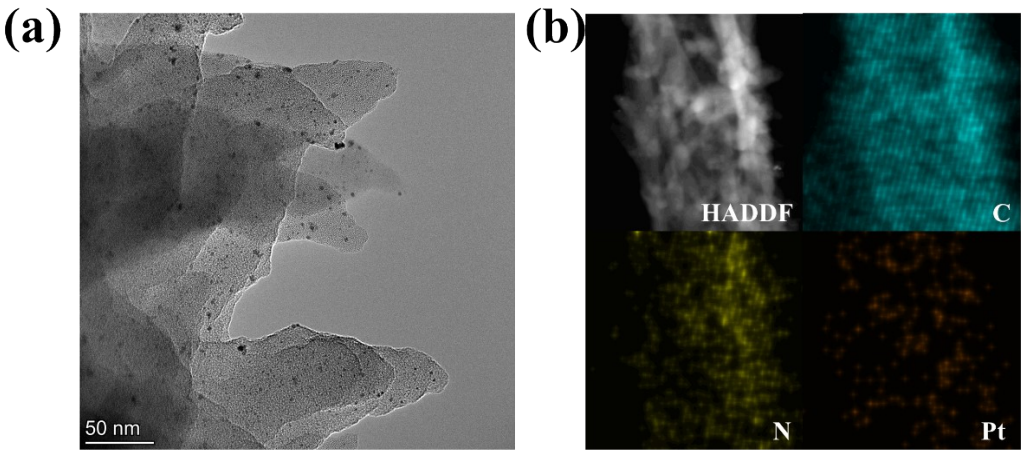

Fig. S22. TEM (a) and EDX elemental mapping (b) images of recovered Pt @ Py-COF from recycling experiment.

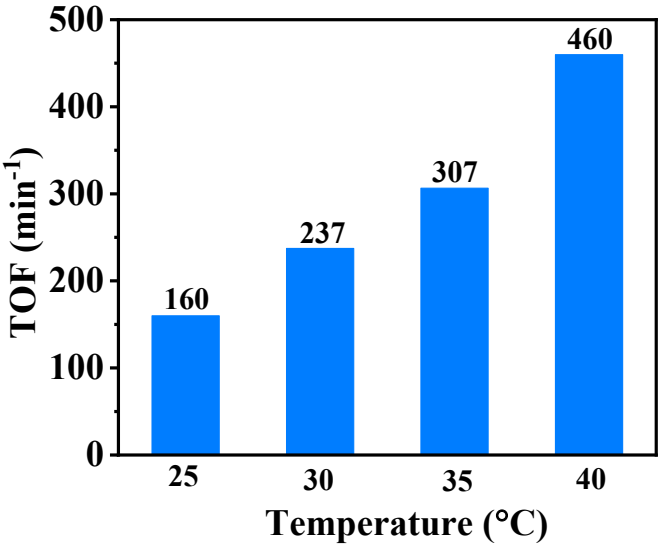

Fig. S23. TOF of H_2 evolution from NH_3BH_3 over Pt@Py-COF at a series of temperature (25, 30, 35 and 40 ℃) (with the conditions of catalysts 10mg, AB 31mg, DI water 5mL).

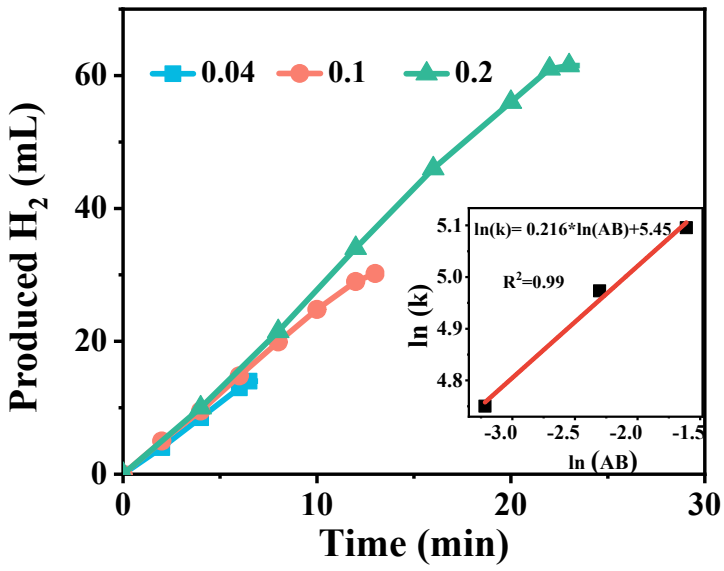

Fig. S24. Kinetics curve of H_2 evolution from AB over Pt@Py-COF at different concentration of AB (inset: the corresponding Arrhenius plots)

Section 4. Liquid ^{1}H and ^{13}C NMR spectra of monomers

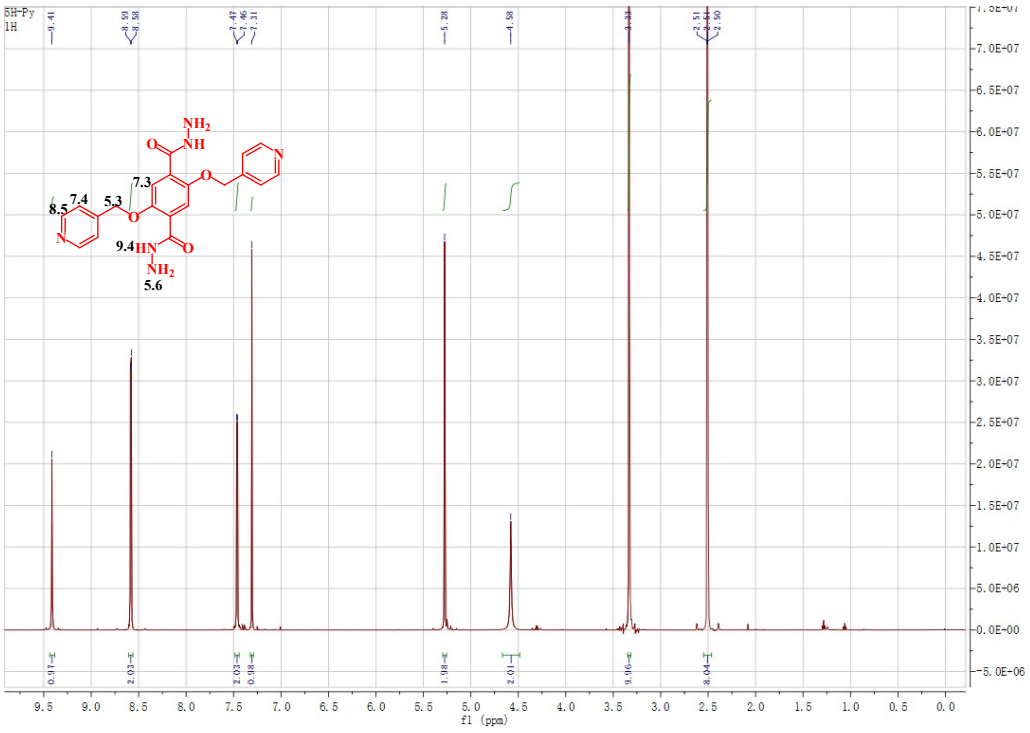

Liquid ^{1}H spectra of PyTH

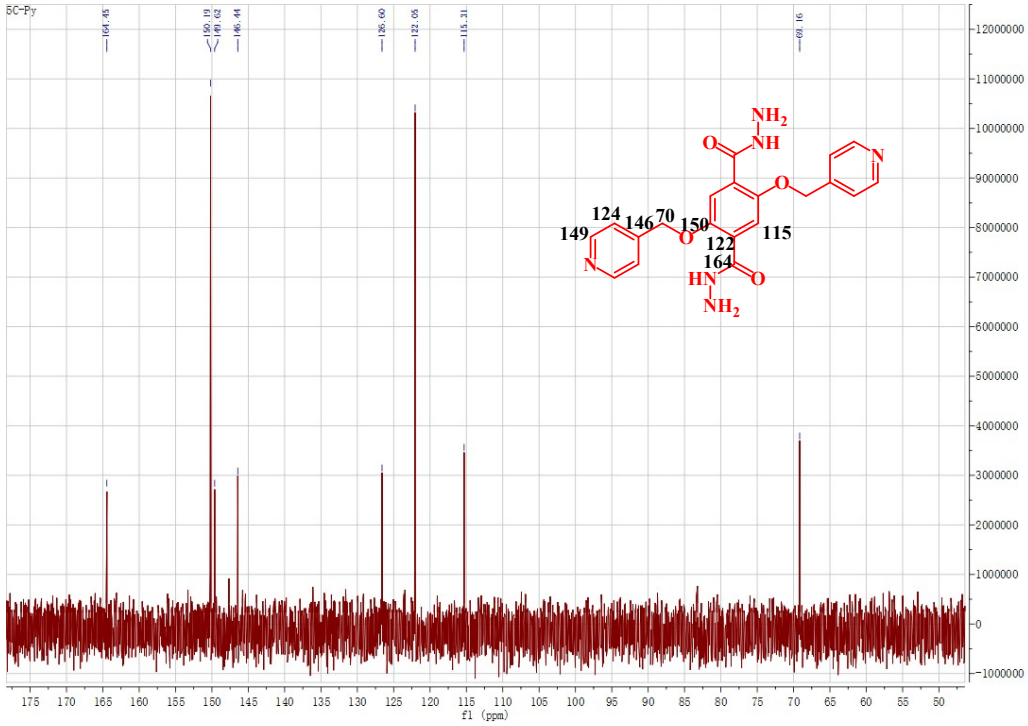

Liquid ^{13}C NMR spectra of PyTH

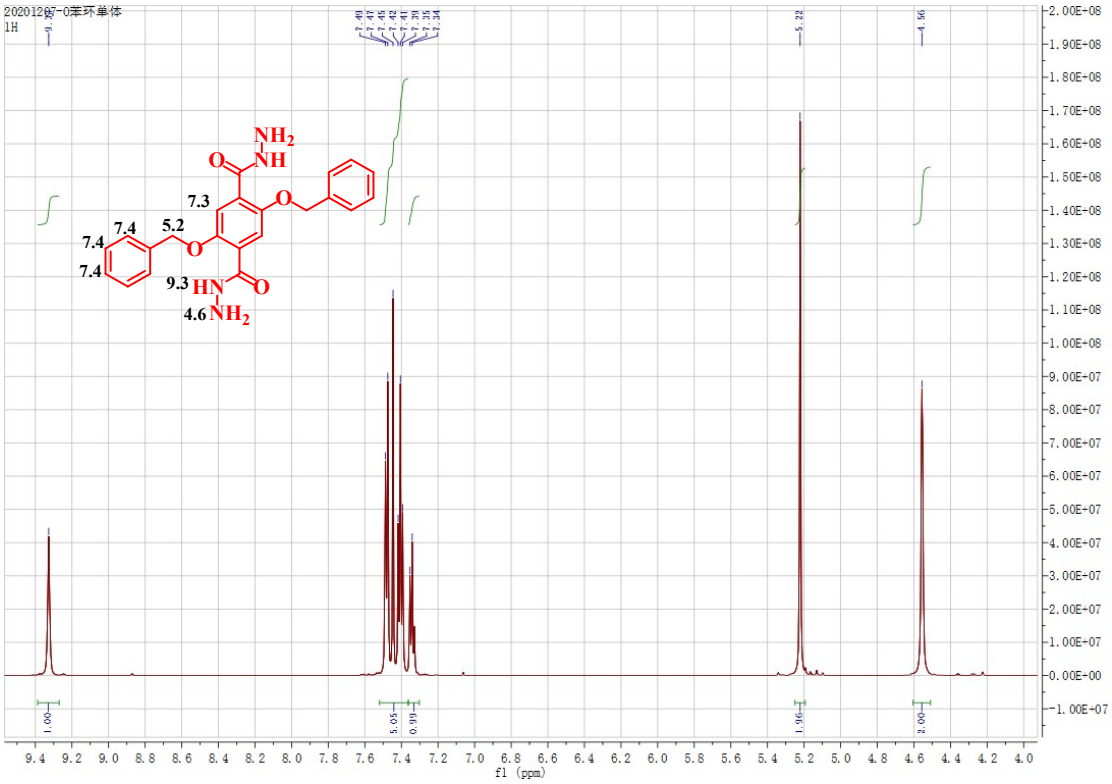

Liquid ^{1}H spectra of BzTH

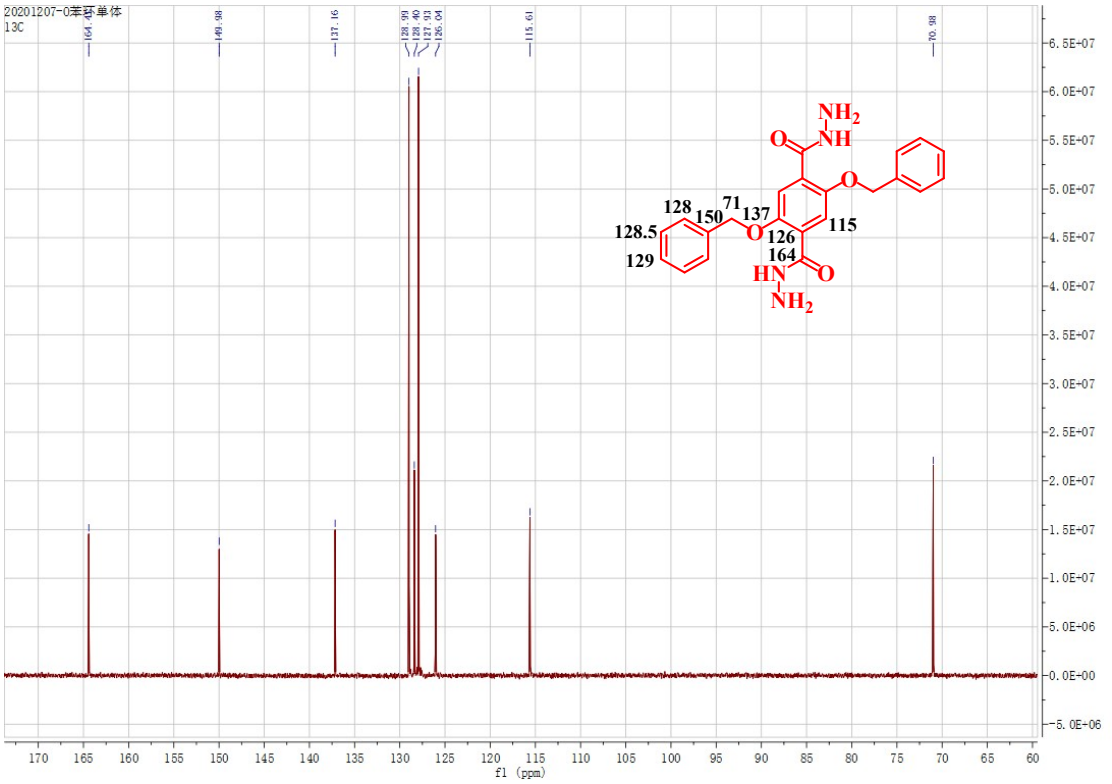

Liquid ^{13}C NMR spectra of BzTH

References

1 M. Chandra and Q. Xu, *J. Power Sources*, 2006, **156**, 190-194.

2 M. Chandra and Q. Xu, *J. Power Sources*, 2007, **168**, 135-142.

3 X. Zhao, Y. Fu, C. Yao, S. Xu, Y. Shen, Q. Ding, W. Liu, H. Zhang and X. Zhou, *ChemCatChem,* 2019, **11**, 2362-2369.

4 H. Zhao, G. Yu, M. Yuan, J. Yang, D. Xu and Z. Dong, *Nanoscale*, 2018, **10**, 21466-21474.

5 A. Uzundurukan and Y. Devrim, *Int. J. Hydrogen Energy*, 2019, **44**, 26773-26782.

6 W. Chen, W. Fu, G. Qian, B. Zhang, Chen, X. Duan and X. Zhou, *iScience*, 2020, **23**, 100922.

7 Y. Hu, Y. Wang, Z.-H. Lu, X. Chen and L. Xiong, *Appl. Surf. Sci.*, 2015, **341**, 185-189.

8 J. R. Deka, C. S. Budi, C. H. Lin, D. Saikia, Y. C. Yang and H. M. Kao, *Chemistry*, 2018, **24**, 13540-13548.